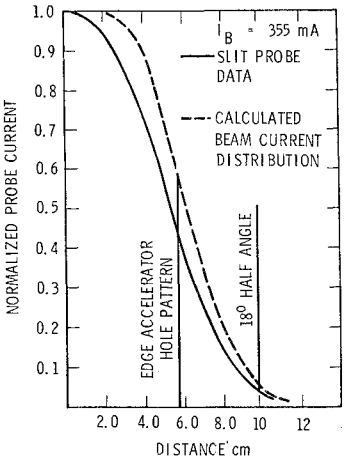

Fig. 4 Radial ion beam distribution.

Environmental Testing

Environmental testing of the thruster at the engineering model stage includes a vibration test and an operation test. The vibration test was conducted along three mutually-perpendicular and three random axes of sinusoidal vibration. After successful vibration, the thruster underwent a break-in test of 500 on-off cycles and 1000 hr of full-thrust operation. Each cycle consists of four different periods: a 2 hr full thrust operational period, a 15 min bakeout period, a 15 min "off" period in which all power was removed from the thruster, and a 30 min warmup and vaporizer stabilization period. Thrust vectoring and beam probing were conducted periodically during the test.

During the 304th cycle, an anode feed line failure was experienced, interrupting the test. The thruster was examined for signs of wear, but no evidence of ion erosion was found in the discharge chamber structure or on the magnets and pole piece. No erosion was seen on the cathode, anode feed ring, screen electrode, or forward pole piece. The orifice diameters of the cathode and feed ring were measured and found to match with those taken before the test.

Examination of the accelerator electrode indicated that direct impingement ions had sputtered some material away on the side of the apertures radially outward from the centerline of the thruster. The appearance, position, and symmetry of the erosion suggest the individual accelerator apertures were originally located too far in toward the centerline. The direct impingment erosion observed is believed to have resulted from a wearing-in of the accelerator to fit the ion beams, ion machining the electrode (R3). Normal charge exchange erosion was observed between apertures. A linear extrapolation indicates the webs would be penetrated in 12,000 hr; electrode life should be in excess of 20,000 hr. The thruster was refurbished with a new anode feed ring. All other thruster components remain the same. After refurbishing, the thruster underwent an additional 200 cycles of break-in testing. Post test analysis is still in progress, however no obvious additional wear has been identified.

References

[1] James E., Dillon, T., Gant, G., Jan, L., Trump, G. and Worlock, R., "A One Millipound Cesium Ion Thruster System," AIAA Paper 70-1149, Stanford, Calif., 1970.

[2] Sohl, G. and Fosnight, V.V., "Thruster Vectoring of Ion Engines," *Journal of Spacecraft and Rockets*, Vol. 6, Feb. 1969, pp. 143-147.

[3] Banks, B., "8 cm Mercury Ion Thruster System Technology," AIAA Paper 74-1116, San Diego, Calif., 1974.

Insulation Requirements for Liquid-Fueled Ramjets with Superalloy Motor Cases

Asa K. Fulton* and Jose I. Gonzalez†
Martin Marietta Aerospace, Orlando, Fla.

Nomenclature

A, B	= coefficients in Eq. (2)
G	= thermal conductance from flame to skin
h	= film coefficient
k	= thermal conductivity
M	= Mach number
S	= thickness
T	= temperature
ϵ	= skin emissivity
σ	= Stefan-Boltzmann constant
τ	= flight time
ρC_p	= heat capacity

Subscripts

aw	= adiabatic wall
c	= combustor
eff	= effective
o	= external
s	= space

RAPID graphical methods have been developed for estimating the minimum internal insulation required to protect ramjet motor cases on vehicles cruising at Mach numbers between 3.0 and 5.0 at altitudes between 40 kft and 100 kft. The motor bottle structure is assumed to be made of a superalloy capable of withstanding temperatures up to 2200° R, and the insulation is assumed to be a stable char or a nonablating material.

Two configurations have been considered. The first is where the motor bottle is the outer surface of the vehicle and is therefore subject to external aerodynamic heating, radiation cooling, solar heating, and possible nuclear thermal environments. Equilibrium conditions are rapidly achieved for the normal flight environment. Nuclear thermal effects, which dissipate rapidly, are superimposed on it. The graphical solution discussed in the following solves for a structural equilibrium temperature of 2040°R to allow a margin for a possible nuclear thermal environment. The governing equations are developed as:

Heat from flame to skin = Heat from skin to environment

$$(h_c^{-1} + S/k)^{-1} (T_c - T_{case})$$

$$= h_o (T_{case} - T_{aw}) + \sigma\epsilon (T_{case}^4 - T_s^4) \quad (1)$$

$$G_{eff} = Ah_o + B\epsilon \quad (2)$$

The adiabatic wall temperature and flame temperature are approximated in Fig. 1 for a typical ramjet. Coefficients A and B of Eq. (2) are then as shown in Fig. 2, and typical ex-

Received January 22, 1975; revision received March 24, 1975.
Index categories: LV/M Aerodynamic Heating; Airbreathing Propulsion, Supersonic.

*Senior Engineer, Aerophysics Department, Aeromechanical Division.
†Professional Staff, Aerophysics Department, Aeromechanical Division. Associate Fellow AIAA.

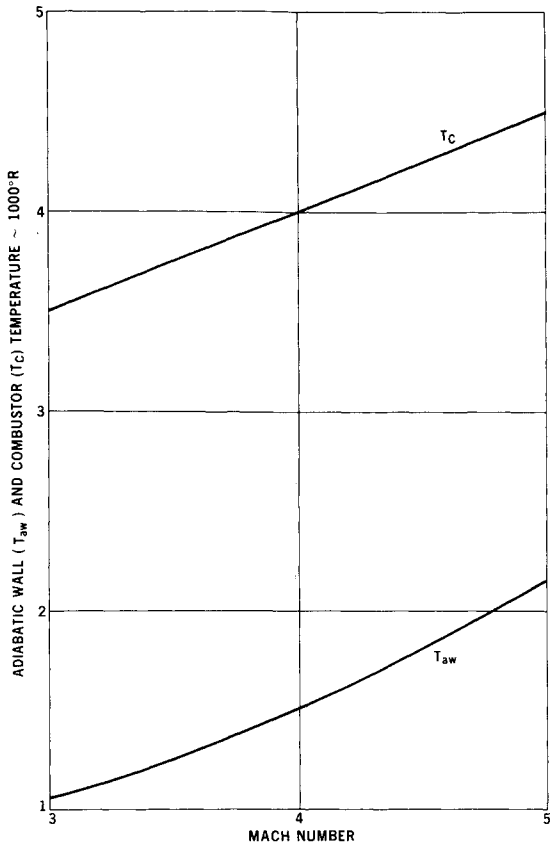

Fig. 1 Adiabatic wall and combustor temperature as a function of Mach number.

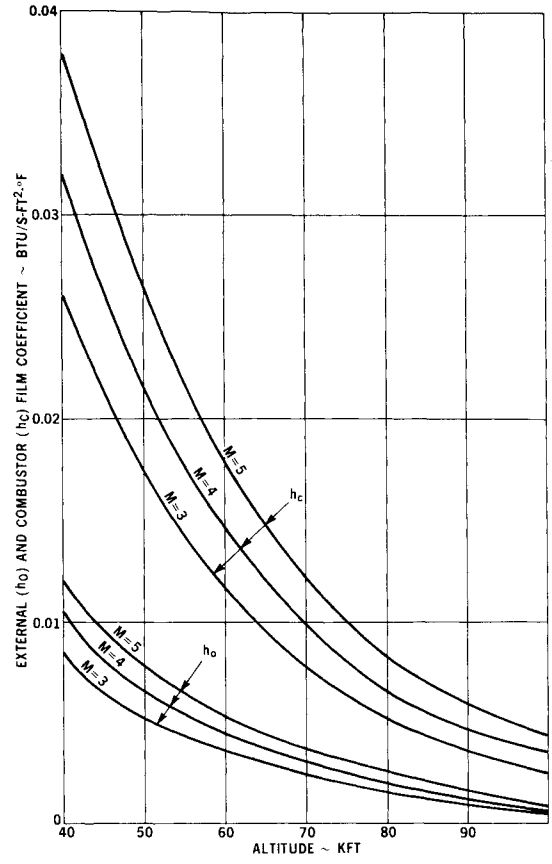

Fig. 3 External and combustor film coefficient as a function of altitude.

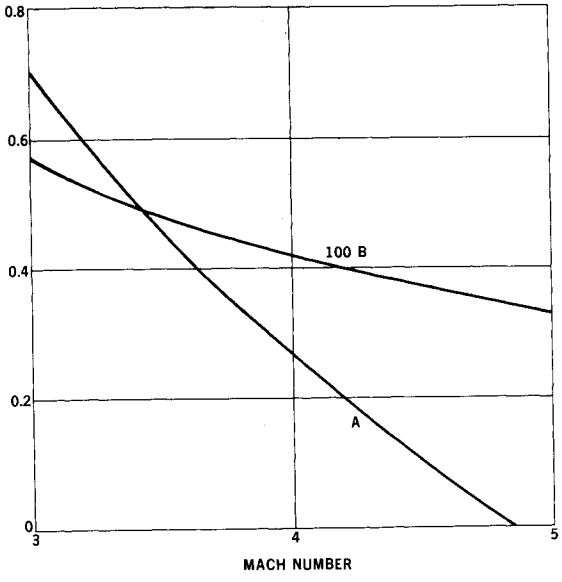

Fig. 2 Convective and radiative conductance coefficients as a function of Mach number.

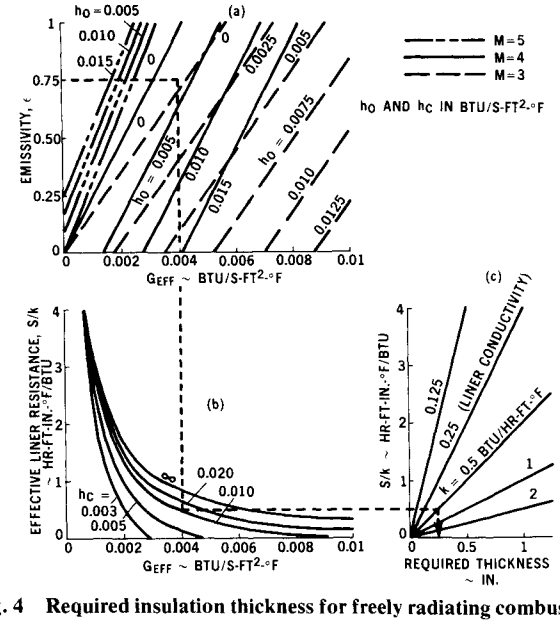

Fig. 4 Required insulation thickness for freely radiating combustor.

ternal and combustor heat transfer coefficients are given in Fig. 3. G_{eff} can now be either calculated directly from Eq. (2), or determined graphically in Fig. 4a.

To determine the required insulation thickness, drop vertically from the point (coordinates of emissivity and h_o) in Fig. 4a to the correct h_c in Fig. 4b, and then go horizontally to the liner conductivity in Fig. 4c. The required thickness is shown on the bottom scale. For example, consider a ramjet cruising at $M=4$, 70 kft, with $\epsilon=0.75$ and $k_{liner}=0.5$ BTU/hr-ft -°F. From Fig. 3, $h_o=0.0031$ BTU/sec-ft²-°F, and h_c = 0.010 BTU/sec-ft² - °F. In Fig. 4a, pick the appropriate point ($G_{eff}=0.004$ BTU/sec-ft² - °F), and drop to $h_c=0.010$ in Fig. 4b, and go across to $k=0.5$ BTU/hr-ft-°F in Fig. 4c. The required thickness is 0.25 in. as read off the bottom scale.

The second configuration is where the combustor wall is embedded in other vehicle structure and not exposed to the vehicle's external environment. Since thermal equilibrium is no longer established, a transient analysis dependent on detailed design information is required. Lacking such information, a conservative estimate of required liner thickness can be made by assuming an adiabatic combustor wall. To ob-

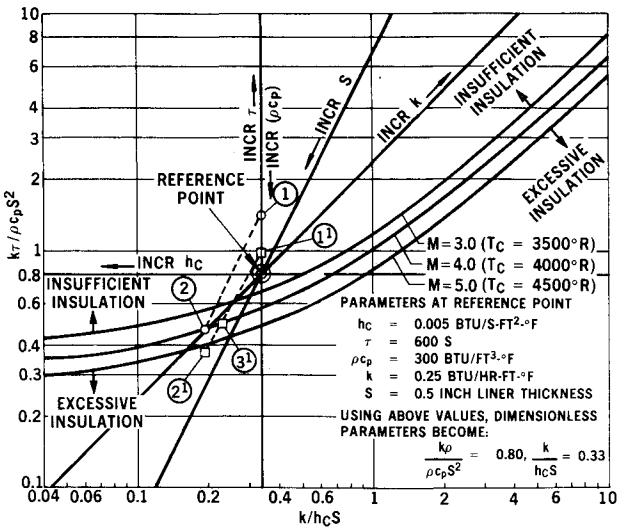

Fig. 5 Required insulation thickness for embedded combustor case.

tain this solution, the same input is required as for the other configuration with the addition of τ, $\rho C_p|_{\text{liner}}$, and $\rho C_p|_{\text{case}}$; and the exception of ϵ and h_o.

Figure 5 is the parametric solution to this problem. For any given insulation thickness and flight environment, the coordinates of a point in the figure can be computed, either with or without $\rho C_p|_{\text{case}}$. This point will fall above the Mach number curve if the insulation is insufficient, and below it if excessive insulation is present. For singular parameter changes, the point moves in the direction indicated by lines passing through the reference point marked "← incr S", "incr k →," etc.

To illustrate this solution, consider the same example as before with $\tau = 525$ sec, $\rho C_p|_{\text{liner}} = 30$ BTU/ft^3-°F, $\rho C_p|_{\text{case}} = 52$ BTU/ft^3 °F, and $S_{\text{case}} = 0.125$ in. Neglecting the case and taking $S_{\text{liner}} = 0.5$ in. as the initial guess, point (1) in Fig. 5 becomes $(k\tau/\rho C_p S^2,\ k/h_c S) = (1.40, 0.333)$. A line through this point parallel to the "incr S" line is constructed; it intersects the $M=4$ curve at (0.465, 0.195) and is labeled (2). The required thickness is

$$S = 0.5[(k/h_c s)|_{(1)}/(k/h_c S)|_{(2)}] =$$

$$0.5\ (0.333/0.195) = 0.85 \text{ in.}$$

If the effect of the case is included, the same general procedure is followed, except that the heat capacity term now varies with liner thickness according to the relation

$$(\rho C_p)_{\text{eff}} = (\rho C_p)_{\text{liner}} + \frac{(\rho C_p S)_{\text{case}}}{S_{\text{liner}}}$$

The points on the plot corresponding to a liner thickness of 0.5 in. [marked (1′)] and 0.85 in. [marked (2′)] are calculated

For (1′):

$$(\rho C_p)_{\text{eff}} = 30 + \frac{52(0.125)}{0.5} = 43$$

$$\frac{k\tau}{\rho C_p S^2} = 1.4\ (30/43) = 0.976$$

$$\left[\frac{k\tau}{\rho C_p S^2},\ \frac{k}{h_c S}\right]_{(1')} = (0.976, 0.333)$$

Similarly for (2′):

$$\left[\frac{k\tau}{\rho C_p S^2},\ \frac{k}{h_c S}\right]_{(2')} = (0.371, 0.195)$$

Lines parallel to the "incr S" line are drawn through these points to the $M=4$ curve. The solution is between these intercepts in approximate proportion to the lengths of the constructed lines. Let $k/h_c S = 0.230$ be considered as one solution coordinate. The corresponding liner thickness is $S = 0.5\ (0.333/0.230) = 0.72$ in. The other coordinate is now calculated, $k\tau/\rho C_{p\text{eff}} S^2 = 0.490$ which happens to be the other coordinate of the $M=4$ curve at $k/h_c S = 0.230$. This, therefore, is the correct solution point marked (3′) in the figure. In this example accounting for the heat capacity of the motor case allows a 15% reduction in liner thickness.

Response of a Dual-Spin Spacecraft with Flexible Appendages via Modal Analysis

L. Meirovitch* and A.L. Hale†
Virginia Polytechnic Institute and State University, Blacksburg, Va.

Nomenclature

m	$= n \times n$ constant, symmetric inertia matrix for the spacecraft
g	$= n \times n$ constant, skew symmetric gyroscopic matrix for the spacecraft due to Coriolis forces
k	$= n \times n$ constant, symmetric stiffness matrix for the spacecraft due to elastic restoring forces and centrifugal forces
$q(t)$	$= n$-dimensional configuration vector (including rotational and elastic motion)
$f(t)$	$= n$-dimensional generalized force vector
M	$= 2n \times 2n$ "inertia matrix" for the spacecraft
G	$= 2n \times 2n$ "gyroscopic matrix" for the spacecraft
$x(t)$	$= 2n$-dimensional state vector
$X(t)$	$= 2n$-dimensional generalized force vector [associated with $x(t)$]
ω_r	= natural frequency of oscillation of the spacecraft
y_r, z_r	= natural modes belonging to ω_r
I	= moment of inertia of entire spacecraft in the nominal configuration about a transverse axis
J	= moment of inertia of the rotor R
Ω	= spin velocity of the rotor
θ_1, θ_2	= attitude angles of the despun section
μ	= single mass simulating the simplified appendage
r_3	= distance from the system mass center to μ
u_1, u_2	= elastic displacements of μ
σ_o	= natural frequency of simplified appendage
v_1, v_2	= elastic velocities of μ
Ω_1, Ω_2	= nutational velocities
$\hat{M}$	= moment impulse

Introduction

EARLY spacecraft were relatively small in size and could be idealized as rigid bodies. In certain cases, the mission required that the spacecraft maintain a given orientation in space, a requirement that could often be met by means of spin stabilization. However, energy

Received April 11, 1975; revision received May 13, 1975.
Index categories: Spacecraft Attitude Dynamics and Control; Structural Dynamic Analysis.

*Professor, Department of Engineering Science and Mechanics. Associate Fellow AIAA.
†Graduate Research Assistant, Department of Engineering Science and Mechanics.